Environmental Science and Pollution Research (2019) 26:16568–16576
https://doi.org/10.1007/s11356-019-05050-z

RESEARCH ARTICLE

Simultaneous removal of nitrate/phosphate with bimetallic nanoparticles of Fe coupled with copper or nickel supported on chelating resin

Zhanhui Shen[1] · Xinyi Dong[1] · Jialu Shi[1,2] · Yuanhao Ma[1] · Daoru Liu[1] · Jing Fan[1]

Received: 22 January 2019 / Accepted: 1 April 2019 / Published online: 13 April 2019

Abstract

Given the prevalence of nitrate and phosphate in surface and groundwater, it is important to develop technology for the simultaneous removal of nitrate and phosphate. In this study, we prepared the bimetallic nanoparticles of Fe coupled with copper or nickel supported on chelating resin DOW 3N (D-Fe/Ni and D-Fe/Cu) for removing nitrate and phosphate simultaneously. XPS profiles revealed that Cu has better ability than Ni to increase the stability of Fe nanoparticles and prevent nZVI from oxidation. The results showed that nitrate removal efficiencies by D-Fe/Ni and D-Fe/Cu were 98.7% and 95.5%, respectively and the phosphate removal efficiencies of D-Fe/Cu and D-Fe/Ni were 99.0% and 93.0%, respectively. Besides adsorption and coprecipitation as reported in previous studies, the mechanism of phosphate removal also includes the adsorption of the newly formed polymeric ligand exchanger (PLE). Moreover, in previous studies, the presence of phosphate had significant negative effects on the reduction of nitrate. However, in this study, the removal efficiency of nitrate was less affected with the increasing concentration of phosphate for D-Fe/Cu. This was mainly because D-Fe/Cu had higher adsorption capacity of phosphate due to the newly formed PLE according to the XPS depth profile analysis.

Keywords Resin · Bimetallic nanoparticles · Nanoscale zero-valent iron · Nitrate · Phosphate

Introduction

Excessive nutrients (nitrate and phosphate) are among the most concerning widespread contaminants in the surface and groundwater (He et al. 2018; Khalil et al. 2017). It has become a problem throughout the world that the increased amount of nutrients has caused the eutrophication of water bodies. This phenomenon will bring about the deletion of oxygen that leads to fish death and effects on aquatic environment. It is a serious problem for different purposes of water uses. Excess phosphorus in water bodies could cause eutrophication when the concentration of phosphorus in lakes exceeds 0.02 mg L^{-1} (Loganathan et al. 2014). On the other hand, excessive nitrate exposure can cause cancer and blue baby disease in infants (Lundberg et al. 2004). The World Health Organization (WHO) has restricted the allowed concentration of nitrate under 50 mg NO_3^-/L.

Nanoscale zero-valent iron (nZVI) has been receiving a lot of attention in wastewater treatment and environmental applications in the last two decades due to its high surface area to volume ratio, high reactivity, environmental friendliness, and cost effectiveness (Wu et al. 2014; Zheng et al. 2008). nZVI has been shown to be effective in removing nitrate (Dong et al. 2018; Khalil et al. 2018). Nitrite is regarded as an intermediate and ammonium is the main reduction product. Besides high reductive efficiency, nZVI particles show good sorptive characteristics. A few literatures discussed the removal of

Responsible editor: Bingcai Pan

Electronic supplementary material The online version of this article (https://doi.org/10.1007/s11356-019-05050-z) contains supplementary material, which is available to authorized users.

✉ Zhanhui Shen
zhshen@htu.edu.cn

✉ Jialu Shi
shijialu@htu.edu.cn

[1] Key Laboratory for Yellow River and Huai River Water Environmental and Pollution Control, Ministry of Education, Henan Key Laboratory for Environmental Pollution Control, School of Environment, Henan Normal University, Xinxiang 453007, Henan, China

[2] State Key Laboratory of Pollution Control and Resource Reuse, School of the Environment, Nanjing University, 163 Xianlin Avenue, Nanjing 210046, China

phosphate using nZVI (Sleiman et al. 2017; Wen et al. 2014). The mechanism of phosphorus removal by nZVI might include the physical adsorption on the surface of nZVI and coprecipitation (Liu et al. 2014). Given the prevalence of nitrate and phosphate in many regions, it is important to develop technology for the simultaneous removal of nitrate and phosphate. Very few literatures reported the simultaneous removal of nitrate and phosphate by nZVI and Fe/Ni bimetallic nanoparticles (He et al. 2018; Khalil et al. 2017). However, the presence of phosphate seriously inhibited nitrate reduction. When the concentration of phosphate was 20 mg L^{-1}, the removal efficiency of nitrate was only about 50% (He et al. 2018). So, it is important to adopt effective measures and minimize the negative influence of phosphate to nitrate reduction in order to remove nitrate and phosphate simultaneously.

In previous studies, researchers prepared polymeric ligand exchanger (PLE) by loading metal ion Cu^{2+} onto chelating resin to removal phosphate (as HPO_4^{2-}) (An et al. 2013; Zhao and Sengupta 1998). PLE is a promising sorbent that sorbs chemicals primarily based on its ligand properties. It has been observed that chelating resins with pyridine-nitrogen atoms can be used as an excellent metal carrier polymer, and the nitrogen donor atoms in the chelating polymers interact with various metal ions and have the highest affinity for Cu^{2+} according to the Irving-Williams series (Henry et al. 2004). The PLE was very selective toward phosphate and anion exchange accompanied by Lewis acid-base interaction is the underlying reason for PLE's enhanced affinity toward phosphate.

Chelating resin DOW 3N (DOWEX™ M4195), which is composed of a polystyrene cross-linked with divinyl benzene backbone and bis(2-pyridylmethyl)amine functional groups, was an excellent metal hosting polymer. Many researchers used chelating resin DOW 3N as the metal hosting polymer to prepare PLE (An et al. 2005; Du et al. 2018). We have used the chelating resin DOW 3N as the supporting material for nZVI and Fe-based bimetallic nanoparticles (Shi et al. 2018, 2016, 2013). The results indicated that the supported nZVI and bimetallic nanoparticles on DOW 3N showed good performance on nitrate reduction. In this study, we investigated the removal of nitrate and phosphate using iron-based bimetallic nanoparticles supported on chelating resin DOW 3N. In the nitrate reduction process, the iron-based bimetallic nanoparticles were oxidized to metal ion, which can form a new (PLE) with a high capacity for phosphate. This is the reason why we choose DOW 3N as the support of iron-based bimetallic nanoparticles to simultaneously remove nitrate and phosphate.

The objectives of this study are to (1) investigate the interplay between nitrate and phosphate; (2) choose appropriate bimetallic nanoparticles to reduce the impact of phosphate to nitrate removal; (3) discuss the mechanism of simultaneously removing nitrate and phosphate.

Materials and methods

Chemicals and materials

The following chemical reagents and materials were used: ferric sulfate ($Fe_2(SO_4)_3$), nickel chloride hexahydrate ($NiCl_2{\cdot}6H_2O$), copper chloride dehydrate ($CuCl_2{\cdot}2H_2O$), ethyl alcohol, sodium borohydride ($NaBH_4$), sodium nitrate ($NaNO_3$), potassium dihydrogen phosphate (KH_2PO_4). All chemicals are of analytical grade and applied as delivered without further purification. DOW 3N (DOWEX™ M4195) was purchased from Sigma Aldrich. Nitrogen gas was purged into all prepared solutions for deoxygenation.

Synthesis of stabilized nanoscale zero-valent iron particles with Ni and Cu

In the synthesis procedure of stabilized bimetallic particles of Fe coupled with copper and nickel, a specific mass of DOW 3N was first mixed with Fe(III) solution (3 g L^{-1} Fe(III)). Then, the supernatant was decanted, and the resin spheres (DOW 3N-Fe^{3+}) were rinsed several times with ultrapure water. DOW 3N-Fe^{3+} was added into Ni^{2+} or Cu^{2+} solution to obtain DOW 3N-Fe^{3+}/Ni^{2+} or DOW 3N-Fe^{3+}/Cu^{2+}. Afterwards, bimetallic Fe/Ni or Fe/Cu nanoparticles immobilized in resin (D-Fe/Ni or D-Fe/Cu) were obtained by injecting DOW 3N-Fe^{3+}/Ni^{2+} or DOW 3N-Fe^{3+}/Cu^{2+} into 100 mL $NaBH_4$ solution (2% in mass), stirring under a N_2 atmosphere for 2 h at 20 °C. After reduction, the synthesized D-Fe/Ni or D-Fe/Cu was rinsed with deionized water and anhydrous ethanol several times.

The amount of Fe, Cu, and Ni loaded onto the DOW 3N was determined by the method in the previous literature (Shi et al. 2016). The results were shown in Table S1.

Characterization

High-resolution transmission electron microscope (HR-TEM) analyses were performed using a JEM-2100 electron microscope at 200 kV with a resolution of 0.23 nm to analyze the micromorphology of D-Fe/Ni and D-Fe/Cu. The surface composition of D-Fe/Ni and D-Fe/Cu was characterized by an X-ray photoelectron spectrometer (ESCALAB 250Xi, Thermo Fisher, USA).

Batch experiments

Experiments for nitrate or phosphate removal

Batch experiments for nitrate reduction or phosphate were carried out in 500-mL three-neck flasks at 25 °C. A certain amount of composites with 2 g supports was added to

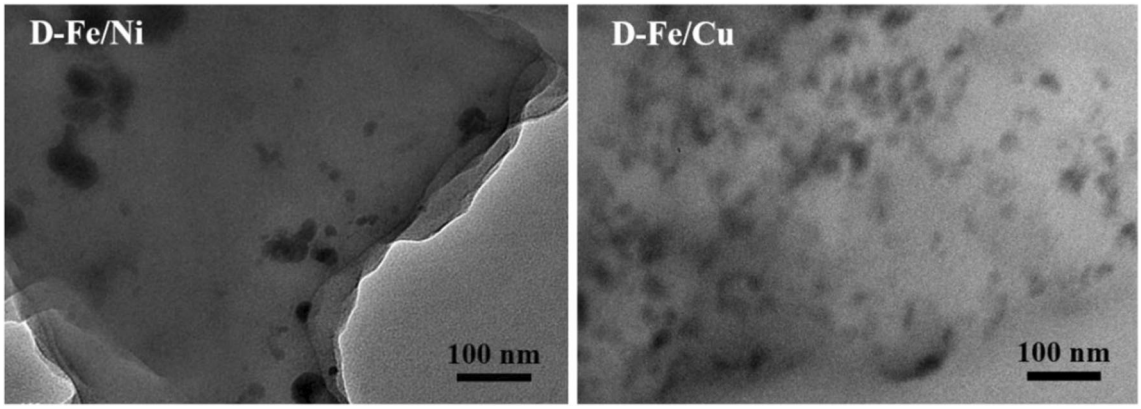

Fig. 1 Transmission electron micrograph images of D-Fe/Ni and D-Fe/Cu

500 mL of 20 mg N L^{-1} nitrate solution or 5 mg P L^{-1} phosphate stirred with a mechanical stirrer. The solution was deoxygenated by a N_2 stream. At specific time intervals, aqueous samples were taken out to determine concentrations of nitrate, nitrite, ammonium, or phosphate after filtering through a 0.22-μm membrane filter. Solution pH was monitored during the reaction process.

The interplay experiments between nitrate and phosphate

To further investigate the effect of one pollutant on another, batch tests were carried out. The concentrations of phosphate-P were 1, 2, and 5 mg L^{-1} with the concentration of nitrate was 20 mg N L^{-1}. Experiments on the influence of nitrate on phosphate removal were conducted at a phosphate concentration of 5 mg P L^{-1} and a nitrate concentration of 20 mg N L^{-1}. The aqueous samples were also collected to determine concentrations of nitrate, nitrite, ammonium, or phosphate after being filtered through a 0.22-μm membrane filter.

Analytical methods

Nitrate, nitrite, and phosphate in solution were determined by ion chromatography (Thermo DIONEX AQUION) with a column of IonPac AS11-HC (4 mm × 250 mm). The mobile phase is 20 mM KOH solution at a flow rate of 1.0 mL min^{-1}. Ammonia was analyzed by a UV-Vis spectrophotometer 2450.

Results and discussion

Characterization of stabilized nanoscale zero-valent iron particles with Ni and Cu

Transmission electron microscope

Figure 1 showed the TEM images of D-Fe/Ni and D-Fe/Cu. We can clearly find that the Fe/Ni and Fe/Cu nanoparticles were well dispersed with no agglomeration. The diameters of Fe/Cu particles were smaller than Fe/Ni particles. The results showed

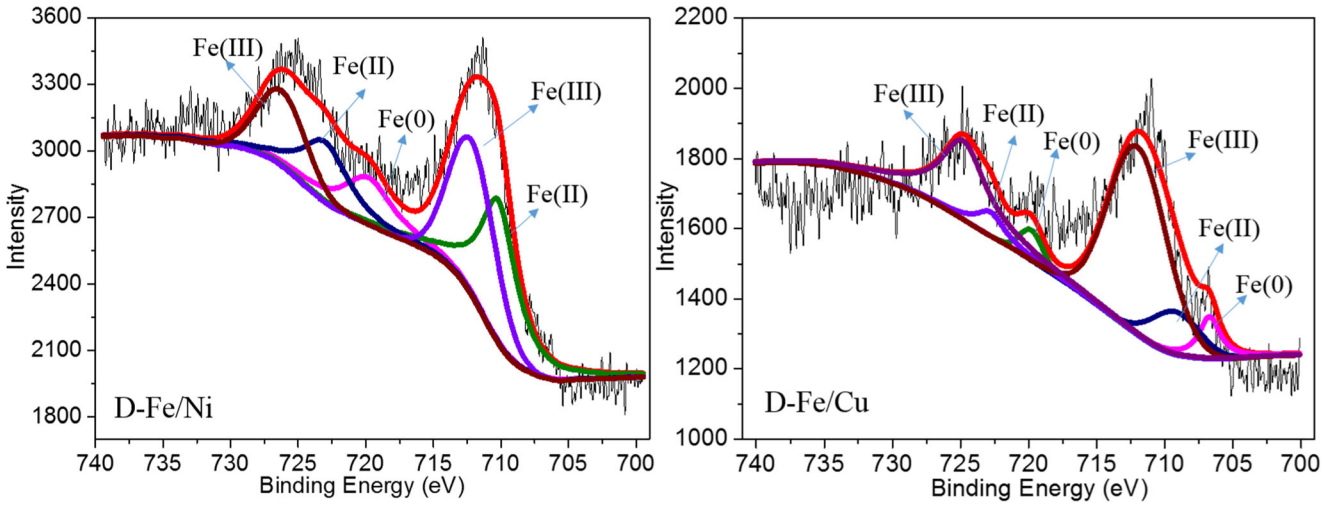

Fig. 2 Fe 2p X-ray photoelectron spectroscopy of D-Fe/Cu and D-Fe/Ni

that resin could inhibit the self-aggregation of nano zero-valent iron and enhanced the dispersibility of nanoparticles.

X-Ray photoelectron spectroscopy

The Fe 2p XPS of D-Fe/Ni and D-Fe/Cu is presented in Fig. 2. Fe mainly existed as Fe(II) (the binding energies of 709.2 eV and 722.8 eV) and Fe(III) (the binding energies of 711.2 eV and 724.8 eV). The results indicated that the surface of iron is mainly composed of an oxide film which might form in the process of preparation and vacuum drying.

Nitrate reduction by supported Fe/Ni and Fe/Cu composites

It has been demonstrated that nitrate was reduced by nZVI to produce nitrite, ammonia, and nitrogen gas (Dong et al. 2018; Khalil et al. 2018). In this study, nitrate reduced by D-Fe/Ni and D-Fe/Cu shows similar phenomena which are shown in Fig. 3. The removal efficiencies of nitrate by D-Fe/Ni and D-Fe/Cu were 98.7% and 95.5%, respectively. Nitrite concentrations increased at the first 1 h and then decreased to lower values. While only few nitrites were observed in the reaction between nitrate and D-Fe/Ni, a considerable amount of nitrite was produced with D-Fe/Cu. It has been reported that Cu exhibited the highest catalytic reduction kinetics of nitrate to nitrite. The higher nitrite concentration generated from D-Fe/Cu was probably due to the higher catalytic reduction activity of nitrate to nitrite with Cu than Ni (Garcia-Segura et al. 2018). Ammonia was the main production both by D-Fe/Ni and D-Fe/Cu.

Phosphate adsorbed by supported Fe/Ni and Fe/Cu composites

The phosphate removal batch study using D-Fe/Cu and D-Fe/Ni was performed and is shown in Fig. 4. The phosphate removal efficiency was more than 80% within 30 min and remained constant after 60 min. The phosphate removal efficiencies of D-Fe/Cu and D-Fe/Ni were 99.0% and 93.0%, respectively. Few studies have reported the removal of phosphate by nZVI due to adsorption and coprecipitation (Sleiman et al. 2017; Zhang et al. 2017). The adsorption of phosphate can be attributed to the metal oxide and hydroxide which were formed during the reaction process. The newly formed metal oxide and hydroxide could adsorb phosphate, due to the strong ligand sorption (of HPO_4^{2-} and $H_2PO_4^-$) through the formation of inner-sphere complexes (Acelas et al. 2015; Hua et al. 2013). In this study, there may be some other mechanisms for the removal of phosphate.

It is known that when iron reacts with water, it forms a thin oxide layer, generating Fe^{2+} and Fe^{3+}. Cu and Ni can also be oxidized and generated Cu^{2+} and Ni^{2+}. These metal ions combined with chelating resin DOW 3N formed a new adsorbent—PLE. Phosphate has three acid ionization constants ($pK_{a1} = 2.1$, $pK_{a2} = 7.2$, and $pK_{a3} = 12.3$), indicating that, at above pH 7.2, the primary species that exists in the aqueous phase is HPO_4^{2-} (see Fig. S2). The final solution pH was around 8, and phosphate mainly existed as HPO_4^{2-} in our study, which was adsorbed preferentially by PLE (An et al.

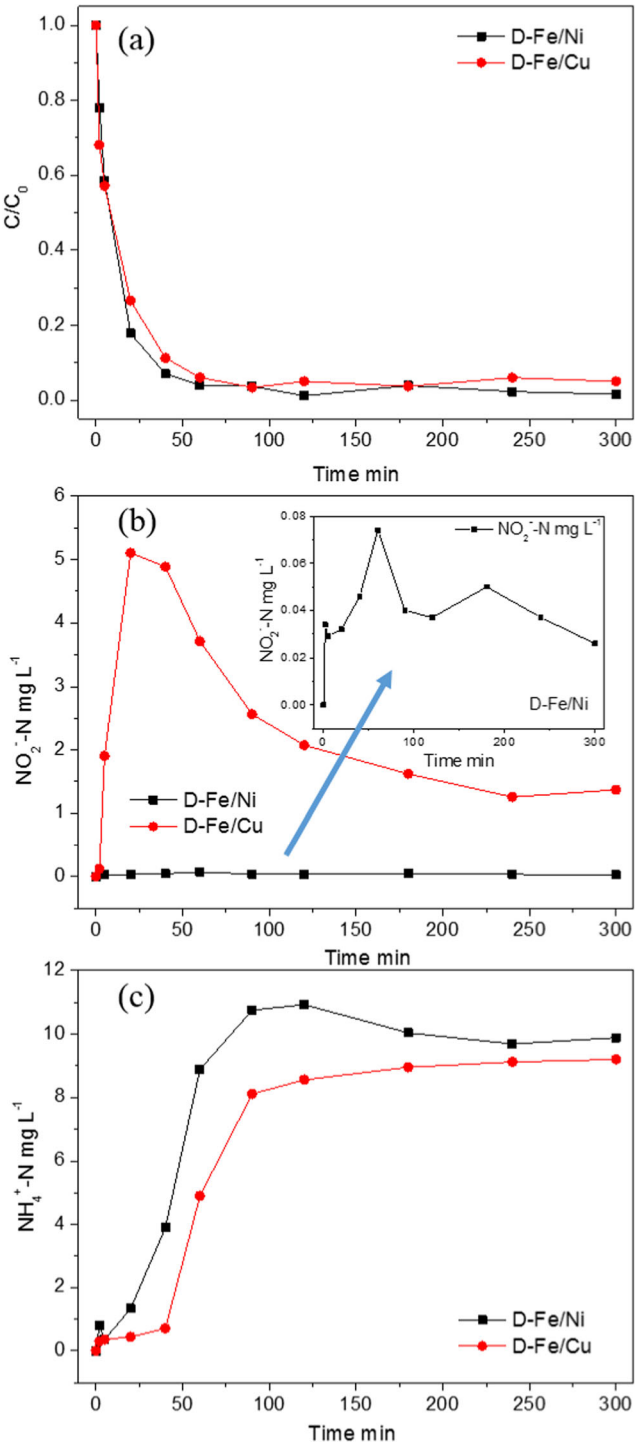

Fig. 3 Nitrate removal by D-Fe/Cu and D-Fe/Ni. **a** C/C_0 of nitrate, **b** NO_2^-N, **c** NH_4^+-N

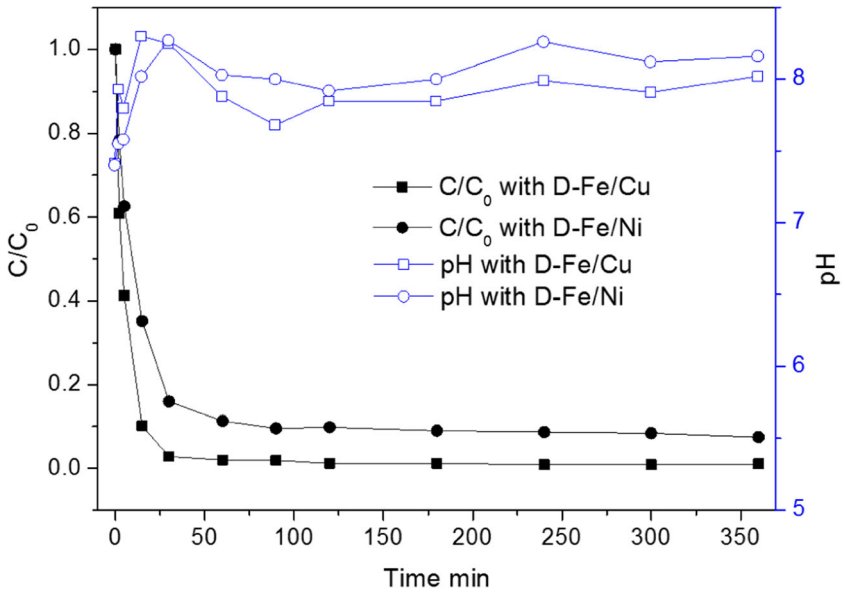

Fig. 4 The adsorption kinetics of phosphate by D-Fe/Cu (black and white squares) and D-Fe/Ni (black and white circles). Filled symbols denote C/C_0 of phosphate and open symbols denote solution pH during the reaction process

2013). D-Fe/Cu has higher phosphate removal efficiency than D-Fe/Ni, demonstrating Cu had higher adsorptive affinity to phosphate than Ni. It has been demonstrated that the capacity of phosphate for PLEs with different metals was following the sequence: $Fe^{2+} < Fe^{3+} < Ni^{2+} < Cu^{2+} > Zn^{2+}$, indicating DOW 3N-Cu has the highest capacity of phosphate (Henry et al. 2004). It is in accord with our study that D-Fe/Cu has a higher phosphate removal efficiency than D-Fe/Ni.

Removal of nitrate and phosphate simultaneously

The effect of phosphate on nitrate reduction

Figure 5 illustrated the effect of phosphate concentration on nitrate reduction. The results showed that there was a negative effect on nitrate reduction by D-Fe/Cu and D-Fe/Ni with the presence of phosphate. The removal efficiencies of nitrate were 95.5% and 98.7% by D-Fe/Cu and D-Fe/Ni, respectively, without the presence of phosphate. With the presence of phosphate, the nitrate removal efficiency was decreased. The data were analyzed by SPSS using one-way ANOVA statistical analysis and it presented a significant negative correlation ($p < 0.05$) with the presence of phosphate both for D-Fe/Cu and D-Fe/Ni (Table S2). However, when the concentration of phosphate increased from 2 to 5 mg L^{-1}, pairwise comparison analysis showed no significant difference ($p = 0.628$) in the removal efficiency of nitrate and the increased concentration of phosphate for D-Fe/Cu (Table S2). This indicated that the removal of nitrate was less affected with the increasing concentration of phosphate for D-Fe/Cu.

To quantitatively evaluate the reduction reactivity, the kinetic model was used to describe the kinetics of nitrate

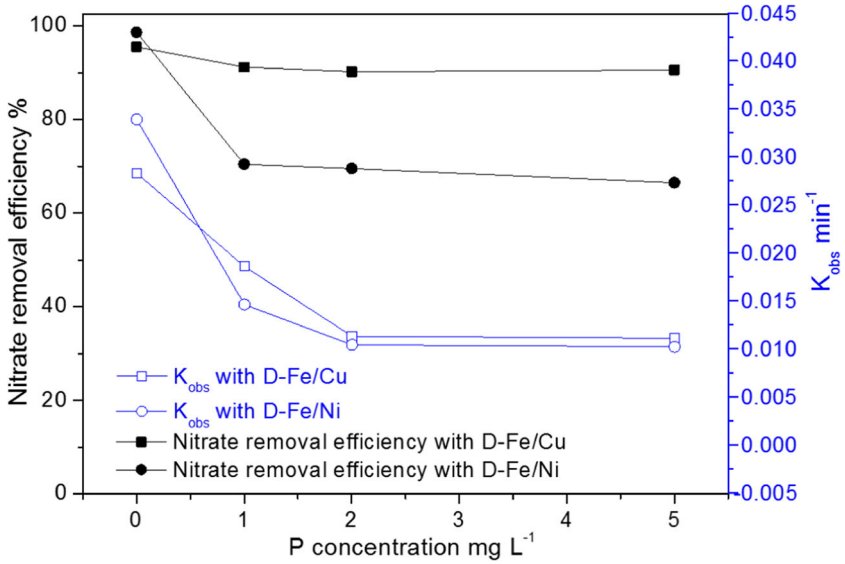

Fig. 5 Nitrate removal by D-Fe/Cu and D-Fe/Ni with different concentrations of phosphate. Filled symbols denote nitrate removal efficiency and open symbols denote K_{obs}

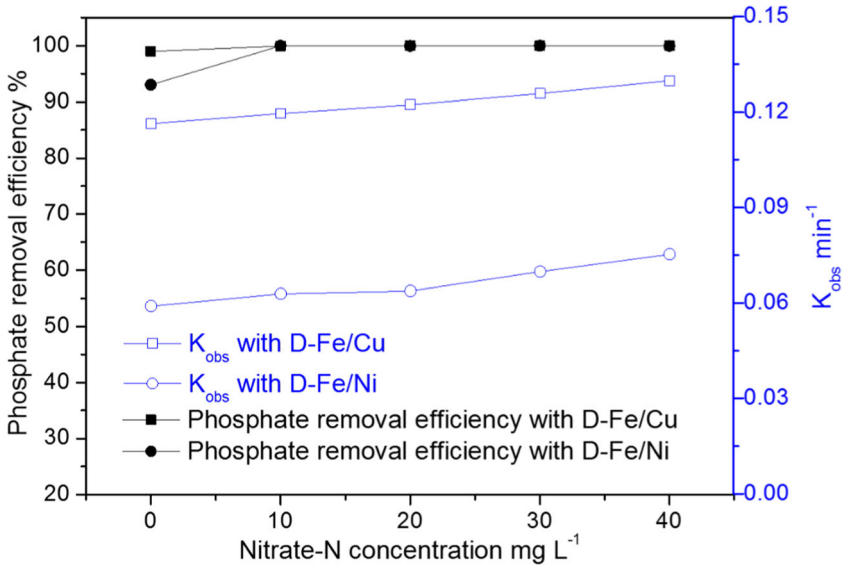

Fig. 6 Phosphate removal by D-Fe/Cu and D-Fe/Ni with different concentrations of nitrate. Filled symbols denote phosphate removal efficiency and open symbols denote K_{obs}

reduction. The results showed that nitrate reduction kinetic was fitted to the pseudo-first-order kinetic model. The pseudo-first-order kinetic model was shown as follows:

$$\frac{d\left[NO_3^-\right]}{dt} = -K_{obs}\left[NO_3^-\right] \quad (1)$$

$$\ln\left(\frac{\left[NO_3^-\right]_0}{\left[NO_3^-\right]_t}\right) = K_{obs}t \quad (2)$$

Where $[NO_3^-]_t$ is the concentration of NO_3^--N (mg L^{-1}) at time t; $[NO_3^-]_0$ is the initial concentration of NO_3^--N (mg L^{-1}); K_{obs} is the observed first-order rate constant (min^{-1}).

The K_{obs} calculated by pseudo-first-order kinetic model was shown in Fig. 5. With the presence of phosphate, the K_{obs} achieved a dramatic decline (from 0.0283 to 0.0186 min^{-1} for D-Fe/Cu and from 0.0339 to 0.0146 min^{-1} for D-Fe/Ni). However, when the concentration of phosphate increased from 2 to 5 mg L^{-1}, the K_{obs} was almost no longer falling. The presence of phosphate has a negative impact on nitrate reduction. It was mainly because phosphate could react with iron nanoparticles and formed iron oxides or hydroxides on the surface of Fe^0, which covered the active sites of Fe/Cu and Fe/Ni nanoparticles and prevented the contact between nitrate and D-Fe/Cu or D-Fe/Ni. Moreover, Fe^{2+}, Fe^{3+}, Cu^{2+}, or Ni^{2+}, which was formed during the reaction of nitrate, also adsorbed phosphate and prevented further corrosion of Fe/Cu or Fe/Ni. As a result, the reduction of nitrate was inhibited. However, the negative effect of phosphate on nitrate reduction by D-Fe/Cu is much smaller than D-Fe/Ni (including removal efficiency and K_{obs}). It is possibly because of the higher adsorption capacity of phosphate for D-Fe/Cu than D-Fe/Ni (Fig. 4). The newly formed adsorbent PLE increased the adsorption sites of phosphate and improved phosphate adsorption capacity, resulting in the negligible effect of phosphate to nitrate reduction.

Phosphate removal performance with and without nitrate addition

Without the presence of nitrate, the phosphate removal efficiencies of D-Fe/Cu and D-Fe/Ni were 99.0% and 93.0%, respectively (see Fig. 4). The removal efficiency increased to nearly 100% both for D-Fe/Cu and D-Fe/Ni with the presence of nitrate. The removal efficiency and K_{obs} of phosphate by D-Fe/Cu and D-Fe/Ni with and without nitrate are shown in Fig. 6. With the presence of nitrate, both the removal efficiency and K_{obs} of phosphate were increased, indicating that the presence of nitrate promoted phosphate removal. The results were analyzed by SPSS using one-way ANOVA statistical analysis in Table S3. The removal efficiency of phosphate presented a significant positive correlation ($p < 0.05$) between with and without the presence of nitrate both for D-Fe/Cu and D-Fe/Ni. However, there were no significant differences for the removal efficiency of phosphate when the concentration of nitrate increased from 10 to 40 mg L^{-1}. The promotive effect of phosphate removal with the presence of nitrate is mainly because the metal (Fe, Cu, or Ni) was oxidized and corroded during the reduction of nitrate, resulting in generation of more metal oxides and hydroxides, or metal ions (Fe^{2+}, Fe^{3+}, Cu^{2+}, or Ni^{2+}), which may react with phosphate via adsorption, coprecipitation, and PLE, thereby promoting phosphate removal.

Proposed mechanism of simultaneous removal of nitrate and phosphate

To further investigate the mechanism of simultaneous removal of nitrate and phosphate by D-Fe/Ni and D-Fe/Cu, XPS combined with ion sputtering for depth profiling was employed after reaction with phosphate and phosphate/nitrate. Fe 2p

high-resolution XPS spectra of D-Fe/Cu and D-Fe/Ni at selected depths are demonstrated in Fig. 7. For all of the samples, iron species existed in the state of different oxidation states Fe(II) and Fe(III). Comparing the Fe 2p XPS of D-Fe/Ni to D-Fe/Cu, the results showed that the Fe(0) area of D-Fe/Ni was much smaller than D-Fe/Cu samples, respectively, which proved that Cu has better ability to increase the stability of nZVI particles and prevent the oxidation of nZVI.

The variations in iron contents with XPS depth profiles, which were obtained from the XPS survey scans in Fig. 7, are shown in Fig. 8. The intensity of the peaks at 706.7 eV and 719.8 eV corresponding to Fe^0 increased with sputter depth. It is worth noting that, for all of the samples, the proportion of Fe^0 on D-Fe/Cu was higher than D-Fe/Ni at the same conditions. It is demonstrated that Cu has better performance for inhibiting the oxidization of Fe^0 than Ni. Moreover, the content of Fe^0 after reaction with nitrate and phosphate was smaller than that after reaction with phosphate for both D-Fe/Cu and D-Fe/Ni in different depths (Fig. 8 a). This was mainly because with the presence of

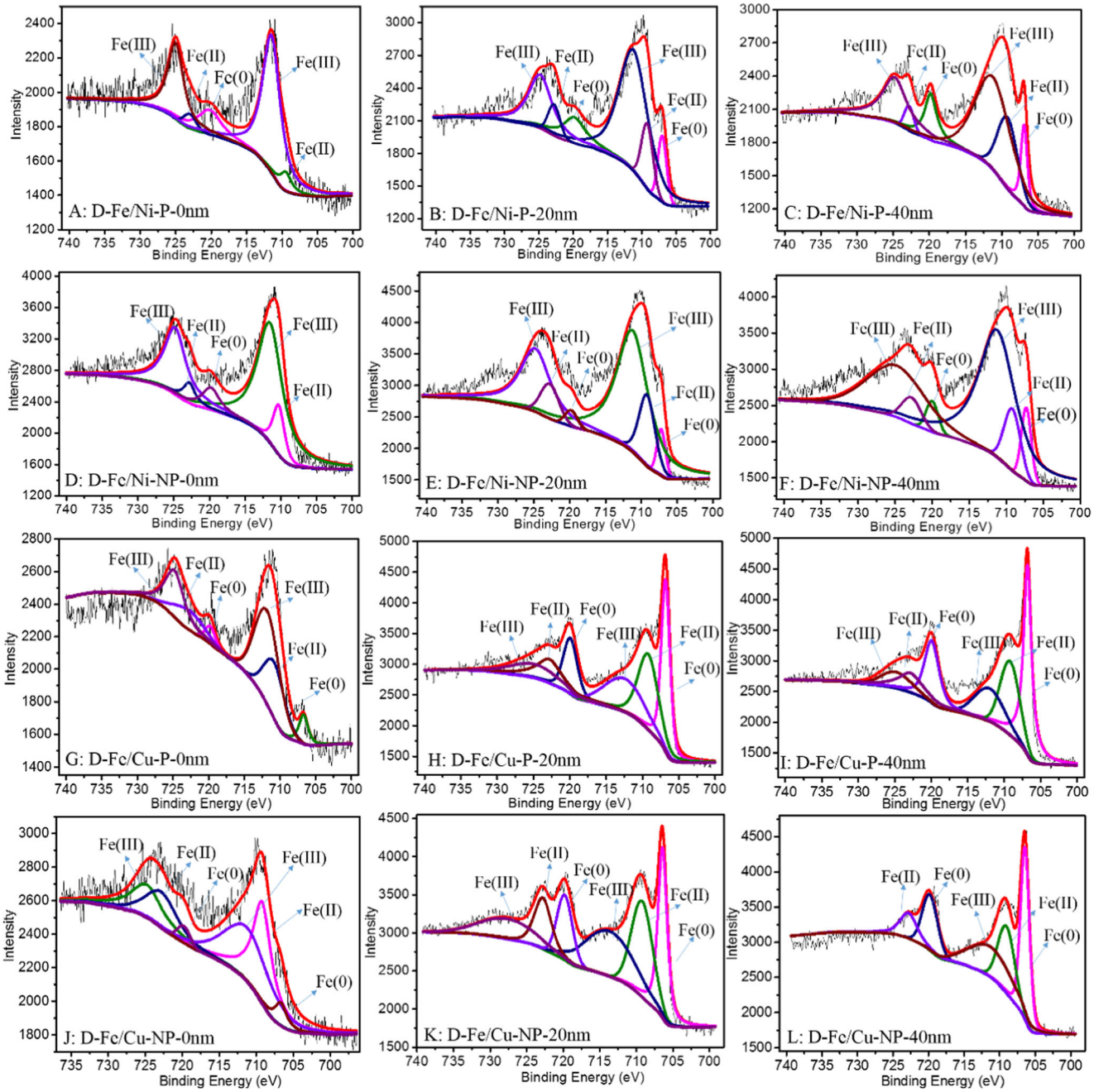

Fig. 7 Fe 2p XPS depth profiling spectra of D-Fe/Ni and D-Fe/Cu after reaction with phosphate (**a**–**c** and **g**–**i**) and phosphate/nitrate (**d**–**f** and **j**–**l**) with different sputtering depths

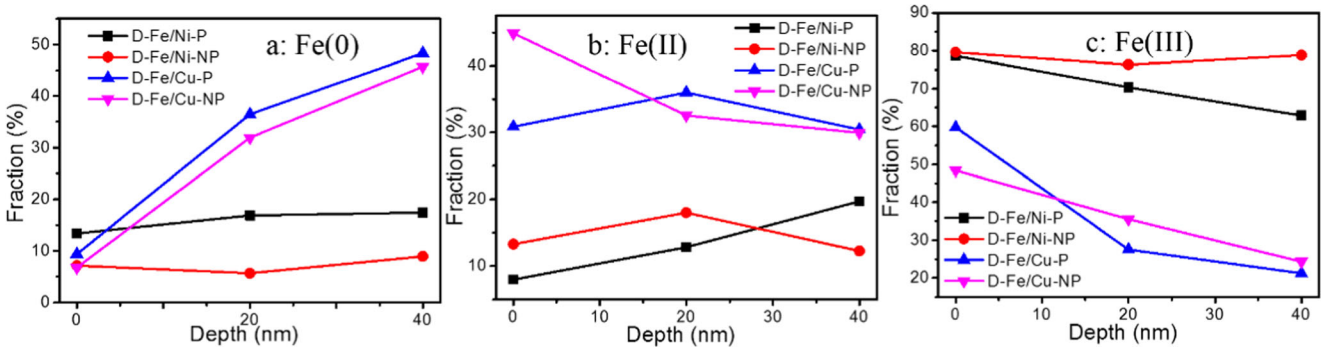

Fig. 8 Fractions of Fe(0), Fe(II), and Fe(III) in different depths of D-Fe/Ni and D-Fe/Cu after reaction with phosphate (D-Fe/Ni-P and D-Fe/Cu-P) and phosphate/nitrate (D-Fe/Ni-NP and D-Fe/Cu-NP), which were calculated from XPS depth spectra

nitrate, the corrosion of Fe^0 was more serious owing to the reaction between Fe^0 and nitrate, and generating more Fe(II) and Fe(III) or iron oxide and hydroxide. This was also the reason for the promotion of phosphate removal with the presence of nitrate.

We speculated the mechanism of simultaneous removal nitrate and phosphate by D-Fe/Ni and D-Fe/Cu as follows:

$$Fe^0 + 2H_2O \rightarrow Fe^{2+} + 2OH^- + H_2 \quad (3)$$

$$Fe^0 + NO_3^- + 2H^+ \rightarrow Fe^{2+} + NO_2^- + H_2O \quad (4)$$

$$3Fe^0 + NO_2^- + 8H^+ \rightarrow 3Fe^{2+} + NH_4^+ + 2H_2O \quad (5)$$

$$2Fe^0 + 3NO_3^- + 6H^+ \rightarrow 2Fe^{3+} + 3NO_2^- + 3H_2O \quad (6)$$

$$2Fe^0 + NO_2^- + 8H^+ \rightarrow 2Fe^{3+} + NH_4^+ + 2H_2O \quad (7)$$

$$2Ni(Cu) + H_2 \rightarrow 2Ni(Cu){-}H_{ads} \quad (8)$$

$$2NO_3^- + 2Ni(Cu){-}H_{ads} + e^- \rightarrow 2Ni(Cu) + 2NO_2^- + OH^- \quad (9)$$

$$NO_2^- + 6Ni(Cu){-}H_{ads} \rightarrow 6Ni(Cu) + NH_4^+ + 2OH^- \quad (10)$$

$$2NO_2^- + 2Ni(Cu){-}H_{ads} \rightarrow 2Ni(Cu) + N_2 + 2OH^- \quad (11)$$

$$Ni^0 + 2H_2O \rightarrow Ni^{2+} + 2OH^- + H_2 \quad (12)$$

$$Cu^0 + 2H_2O \rightarrow Cu^{2+} + 2OH^- + H_2 \quad (13)$$

Presumably, when NO_3^- was reduced into NO_2^- and NH_4^+, Fe^0 was corroded (reactions 3–7). It is indicated from Fig. 8 that iron existed mainly in the form of Fe(III) on D-Fe/Ni while Fe(II) on D-Fe/Cu in Fig. 8 b and c. So, for D-Fe/Cu, the reactions (4)–(5) are dominant, while for D-Fe/Ni, the reactions (6)–(7) are dominant. Ni(Cu) particles can adsorb H_2 produced by nZVI and convert H_2 into Ni(Cu)-H_{ads}. Afterwards, NO_3^- or NO_2^- is adsorbed onto the particles of composite materials and reduced to NH_4^+ or N_2 as shown in reactions (8)–(11).

During the nitrate reaction process, Fe^0 was oxidized into Fe_2O_3/Fe_3O_4, goethite (α-FeOOH) or akaganeite (β-FeOOH), which had a high affinity for phosphate (Almeelbi and Bezbaruah 2012; Li et al. 2018). Moreover, we can find in Fig. 8 that the fractions of Fe^0 and Fe(II) on D-Fe/Cu were higher than D-Fe/Ni, and the fractions of Fe(III) on D-Fe/Cu were smaller than D-Fe/Ni. We have mentioned before that the PLE DOW 3N-Fe^{2+} has a smaller adsorption capacity of phosphate than DOW 3N-Fe^{3+} (Henry et al. 2004); from this point of view, the removal of phosphate of D-Fe/Cu should be smaller than D-Fe/Ni. However, the results showed that the removal of phosphate of D-Fe/Cu was higher than D-Fe/Ni. This was mainly because of the higher adsorption capacity of PLE DOW 3N-Cu^{2+} than DOW 3 N-Ni^{2+} (Henry et al. 2004). It was in accordance with P 2p XPS depth profiling spectra (Fig. S3) that D-Fe/Cu has a higher P 2p peak strength than D-Fe/Ni.

Conclusion

In this study, we prepared the bimetallic nanoparticles of Fe coupled with copper or nickel supported on chelating resin DOW 3N (D-Fe/Ni and D-Fe/Cu) for simultaneous nitrate and phosphate removal. It was confirmed that both D-Fe/Ni and D-Fe/Cu showed high nitrate reduction efficiency and phosphate removal efficiency. XPS profiles indicated that D-Fe/Cu could make Fe^0 more stable than D-Fe/Ni. Batch experiment results indicated that nitrate reduced by D-Fe/Ni and D-Fe/Cu showed similar phenomena and the removal efficiencies of nitrate by D-Fe/Ni and D-Fe/Cu were 98.7% and 95.5%, respectively. The main reduction product of nitrate by D-Fe/Ni was ammonia while those by D-Fe/Cu were nitrite and ammonia. The phosphate removal efficiencies were 99.0% and 93.0% by D-Fe/Cu and D-Fe/Ni, respectively. The mechanism of phosphate removal was adsorption, coprecipitation, and a new adsorbent-PLE which formed during the process of nitrate reduction.

The existence of nitrate promoted phosphate removal while the presence of phosphate inhibited the reduction of nitrate both by D-Fe/Cu and D-Fe/Ni. However, the inhibition of phosphate to nitrate reduction by D-Fe/Cu was smaller than D-Fe/Ni and the removal efficiency of nitrate was almost insusceptible with the presence of phosphate for D-Fe/Cu. It is

possibly because of the higher adsorption capacity of phosphate for D-Fe/Cu than D-Fe/Ni. The simultaneous removal of nitrate and phosphate mechanism involved reduction, adsorption, coprecipitation, and a newly formed adsorbent-PLE.

Funding information This research was financially funded by the postdoctoral science foundation of China (No. 2018M642758), the State Key Laboratory of Pollution Control and Resource Reuse Foundation (No. PCRRF 17034), the Education Department of the Henan Science and Technology Fund Project (No. 16A610009), the State Key Program of National Natural Science of China (No. 51438008 and No. 51604099).

References

Acelas NY, Martin BD, López D, Jefferson B (2015) Selective removal of phosphate from wastewater using hydrated metal oxides dispersed within anionic exchange media. Chemosphere 119:1353–1360

Almeelbi T, Bezbaruah A (2012) Aqueous phosphate removal using nanoscale zero-valent iron. J Nanopart Res 14:900–914

An B, Steinwinder TR, Zhao D (2005) Selective removal of arsenate from drinking water using a polymeric ligand exchanger. Water Res 39: 4993–5004

An B, Nam J, Choi JW, Hong SW, Lee SH (2013) Enhanced phosphate selectivity from wastewater using copper-loaded chelating resin functionalized with polyethylenimine. J Colloid Interface Sci 409: 129–134

Dong L, Lin L, Li Q, Huang Z, Tang X, Wu M, Li C, Cao X, Scholz M (2018) Enhanced nitrate-nitrogen removal by modified attapulgite-supported nanoscale zero-valent iron treating simulated groundwater. J Environ Manag 213:151–158

Du HX, Lung CYK, Lau TC (2018) Efficient adsorption, removal and recovery of phosphate and nitrate from water by a novel lanthanum(iii)-Dowex M4195 polymeric ligand exchanger. Environ Sci-Wat Res 4:421–427

Garcia-Segura S, Lanzarini-Lopes M, Hristovski K, Westerhoff P (2018) Electrocatalytic reduction of nitrate: fundamentals to full-scale water treatment applications. Appl Catal B Environ 236:546–568

He Y, Lin H, Dong Y, Li B, Wang L, Chu S, Luo M, Liu J (2018) Zeolite supported Fe/Ni bimetallic nanoparticles for simultaneous removal of nitrate and phosphate: synergistic effect and mechanism. Chem Eng J 347:669–681

Henry WD, Zhao D, SenGupta AK, Lange C (2004) Preparation and characterization of a new class of polymeric ligand exchangers for selective removal of trace contaminants from water. React Funct Polym 60:109–120

Hua M, Xiao L, Pan B, Zhang Q (2013) Validation of polymer-based nano-iron oxide in further phosphorus removal from bioeffluent: laboratory and scaled up study. Front Env Sci Eng 7:435–441

Khalil AME, Eljamal O, Amen TWM, Sugihara Y, Matsunaga N (2017) Optimized nano-scale zero-valent iron supported on treated activated carbon for enhanced nitrate and phosphate removal from water. Chem Eng J 309:349–365

Khalil AME, Eljamal O, Saha BB, Matsunaga N (2018) Performance of nanoscale zero-valent iron in nitrate reduction from water using a laboratory-scale continuous-flow system. Chemosphere 197:502–512

Li N, Tian Y, Zhao J, Zhan W, Du J, Kong L, Zhang J, Zuo W (2018) Ultrafast selective capture of phosphorus from sewage by 3D Fe_3O_4@ZnO via weak magnetic field enhanced adsorption. Chem Eng J 341:289–297

Liu F, Yang J, Zuo J, Ma D, Gan L, Xie B, Wang P, Yang B (2014) Graphene-supported nanoscale zero-valent iron: removal of phosphorus from aqueous solution and mechanistic study. J Environ Sci 26:1751–1762

Loganathan P, Vigneswaran S, Kandasamy J, Bolan NS (2014) Removal and recovery of phosphate from water using sorption. Crit Rev Environ Sci Technol 44:847–907

Lundberg JO, Weitzberg E, Cole JA, Benjamin N (2004) Nitrate, bacteria and human health. Nat Rev Microbiol 2:593–602

Shi J, Yi S, He H, Long C, Li A (2013) Preparation of nanoscale zero-valent iron supported on chelating resin with nitrogen donor atoms for simultaneous reduction of Pb^{2+} and NO_3. Chem Eng J 230:166–171

Shi J, Long C, Li A (2016) Selective reduction of nitrate into nitrogen using Fe–Pd bimetallic nanoparticle supported on chelating resin at near-neutral pH. Chem Eng J 286:408–415

Shi J, Ma Y, Shen Z, Liu D, Long C, Zhang X, Shi J, Wang C (2018) Fe-Pd bimetallic composites supported by resins for nitrate reduction: role of surface functional groups in controlling rate and selectivity. Environ Eng Sci 36:295–304. https://doi.org/10.1089/ees.2018.0204

Sleiman N, Deluchat V, Wazne M, Mallet M, Courtin-Nomade A, Kazpard V, Baudu M (2017) Phosphate removal from aqueous solutions using zero valent iron (ZVI): influence of solution composition and ZVI aging. Colloids Surf A 514:1–10

Wen Z, Zhang Y, Dai C (2014) Removal of phosphate from aqueous solution using nanoscale zerovalent iron (nZVI). Colloids Surf A 457:433–440

Wu X, Lu S, Qiu Z, Sui Q, Lin K, Du X, Luo Q (2014) The reductive degradation of 1,1,1-trichloroethane by Fe(0) in a soil slurry system. Environ Sci Pollut Res 21:1401–1410

Zhang Q, Liu H, Chen T, Chen D, Li M, Chen C (2017) The synthesis of NZVI and its application to the removal of phosphate from aqueous solutions. Water Air Soil Pollut 228:321–331

Zhao D, Sengupta AK (1998) Ultimate removal of phosphate from wastewater using a new class of polymeric ion exchangers. Water Res 32: 1613–1625

Zheng T, Zhan J, He J, Day C, Lu Y, McPherson GL, Piringer G, John VT (2008) Reactivity characteristics of nanoscale zerovalent iron-silica composites for trichloroethylene remediation. Environ Sci Technol 42:4494–4499